Binding of DAPI Analogue 2,5-Bis(4-amidinophenyl)furan to DNA†

Karl Jansen, Per Lincoln, and Bengt Nordén*

Department of Physical Chemistry, Chalmers University of Technology, S-412 96 Göteborg, Sweden

Received December 15, 1992; Revised Manuscript Received April 6, 1993

ABSTRACT: The binding of 2,5-bis(4-amidinophenyl)furan (APF) to calf thymus DNA, $[poly(dA\text{-}dT)]_2$, and $[poly(dG\text{-}dC)]_2$ has been studied with flow linear dichroism and circular dichroism spectroscopy. The electronic excited states of the APF chromophore were first characterized using experimental and quantum mechanical methods: it is shown that the low-energy absorption band (320–400 nm) originates from only a single electronic transition which is polarized along the long axis of the molecule, information that is crucial for the structural interpretation of the linear and circular dichroism spectra of the APF–DNA complexes. By contrast, in the unsymmetric analogue 4′,6-diamidino-2-phenylindole (DAPI) two overlapping transitions, with somewhat divergent polarizations, both contribute to the first absorption band. Upon binding to DNA the spectroscopic behavior of APF strongly resembles that of DAPI. The linear dichroism data show that the drug binds to calf thymus DNA and $[poly(dA\text{-}dT)]_2$ with an angle of 46° ± 2° between its symmetry long axis and the DNA helix axis, confirming that APF, just like DAPI, is an AT-specific minor-groove binder. Upon binding to $[poly(dG\text{-}dC)]_2$, however, the orientation of the long axis is parallel with the plane of the DNA bases, a geometry which excludes binding parallel to the grooves but could be consistent with intercalation. However, a short axis polarized transition is strongly inclined to the base plane and, furthermore, the persistence length of the polynucleotide is markedly reduced, observations that contradict classical intercalation. The circular dichroism spectrum in the low-energy absorption band of APF, upon binding to $[poly(dA\text{-}dT)]_2$, displays a "two mode" behavior similar to that of DAPI, which in DAPI has been ascribed to selective activation of either of its two transitions depending on the DNA conformation. However, in contrast to DAPI, this behavior in APF originates from a single electronic transition only. A plausible explanation of the second "mode", which could apply to the DAPI case as well, is that it is a result of long-range exciton interaction between drug chromophores in the minor groove.

This study concerns the DNA interaction of 2,5-bis(4-amidinophenyl)furan (APF), a drug analogous to the well-known AT-specific minor-groove binder 4′,6-diamidino-2-phenylindole (DAPI) (Figure 1). Aromatic diamidino compounds were early studied for their trypanocidal activity [see, *e.g.*, Ashley *et al.* (1942)], and in an effort to produce better trypanocides numerous diamidino compounds, including APF and DAPI, were synthesized (Dann *et al.*, 1971, 1975). Among the compounds synthesized by Dann *et al.* DAPI has become the most widely used, not as a trypanocide but mainly as a DNA probe, because of its large increase in fluorescence quantum yield upon binding to double helical DNA. DAPI has been exploited, for example, in electrophoresis (Kapuscinski & Yanagi, 1979; Schwartz & Koval, 1989), for cytofluorometry (Brown & Hitchcook, 1989; Chi *et al.*, 1990; Hajduk, 1976; Lee *et al.*, 1984; Russel *et al.*, 1975; Takata & Hirano, 1990; Tijssen *et al.*, 1982; Williamson & Fennel, 1979), and for staining chromosomes (Bella & Gosálvez, 1991; Bernheim & Migierina, 1989; Lin *et al.*, 1977).

DAPI (Nordén *et al.*, 1990; Wilson *et al.*, 1990a) and other aromatic amidines, *e.g.*, netropsin (Zimmer & Wähnert, 1986), berenil (Krey, 1980), and hydroxystilbamidine (Festy & Duane, 1973; Festy *et al.*, 1975), have been found to bind specifically to AT-rich regions of DNA, in which they are accommodated in the minor groove. In the crystal structure of a 1:1 complex between DAPI and the Drew–Dickersson dodecamer DAPI is found at the central AT stretch inserted edgewise into the minor groove (Larsen *et al.*, 1989). The amidino groups of these compounds seem to be crucial for the binding to DNA (Newton, 1967; Wilson *et al.*, 1990b). Despite the fact that the binding properties of DAPI have been studied extensively, there still remain several unanswered important questions as to how DAPI interacts with DNA. More specifically, the appearance of two "modes" seen in the circular dichroism spectrum upon binding DAPI to AT-rich sequences, the one with highest affinity having virtually a very low binding density, has been a matter of debate (Manzini *et al.*, 1983; Kubista *et al.*, 1987; Nordén *et al.*, 1990).

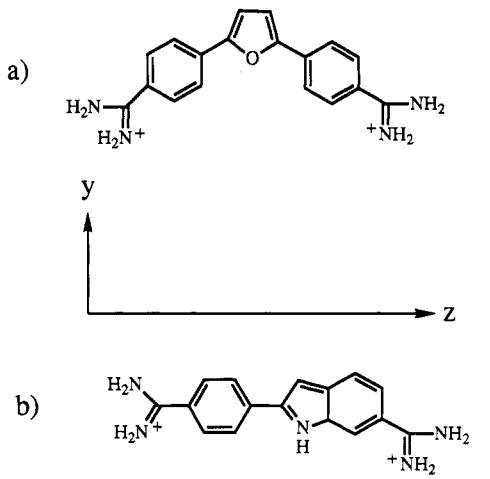

FIGURE 1: Molecular formulas of 2,5-bis(4-amidinophenyl)furan (APF) and 4′,6-diamidino-2-phenylindole (DAPI) with notations for the molecular symmetry (pseudosymmetry) axes.

In contrast to DAPI, APF is C_{2v} symmetric in its planar conformation which greatly facilitates interpretation of its DNA binding properties and spectra. Wilson *et al.* (1990b) have recently proposed APF as a model compound for minor-

† This project was supported by the Swedish Natural Science Research Council.

* To whom correspondence should be addressed.

0006-2960/93/0432-6605$04.00/0

groove binding agents in a study focusing on the origin of groove binding and intercalation.

Dann *et al.* (1975) showed that APF is effective against *Trypanosoma rhodesense*. Das and Boykin (1977) synthesized and studied antiprotozoal effects of APF and other 2,5-bis(4-guanylphenyl)furan compounds. The binding constants of DAPI and APF upon binding to natural duplex DNAs and polynucleotides are of the same order of magnitude, although slightly lower for APF. The lack of the hydrogen-donating NH group in APF has been proposed to be compensated for by a more pronounced curvature of APF compared with DAPI (Wilson *et al.*, 1990b).

In this study we have used linear dichroism (LD) to characterize the binding geometry of APF in its complexes with calf thymus DNA, [poly(dA-dT)]$_2$, and [poly(dG-dC)]$_2$. In order to adequately interpret the LD spectra for the APF–DNA complex when oriented by a shear gradient in a flowing solution, the transition moment directions responsible for the absorption must be known in the molecular framework of the chromophore. To gain such information, we have first studied APF itself, using both experimental and theoretical methods, concentrating on its low-energy absorption bands. The measurements include linear dichroism in stretched poly(vinyl alcohol) film, fluorescence anisotropy, and magnetic circular dichroism.

MATERIALS AND METHODS

Chemicals. All chemicals used were of analytical grade and aqueous solutions prepared with deionized triply filtered water (Millipore). APF was a gift from Doctors B. P. Das and D. W. Boykin who synthesized the compound (Das & Boykin, 1977). Poly(vinyl alcohol) (PVA), obtained as a powder from E. I. du Pont de Nemours Co. (Elvanol 71-30), was hydrolyzed in ethanolic NaOH solution (20% water, refluxing for 10 h) and precipitated in ethanol prior to use. 1,2-Propanediol was purchased from Merck, calf thymus DNA (type I) was purchased from Sigma, and [poly(dA-dT)]$_2$ and [poly(dG-dC)]$_2$ were purchased from Pharmacia. The molar absorptivities used for concentration determinations were 6600 M^{-1} cm^{-1} at 260 nm for calf thymus DNA and [poly(dA-dT)]$_2$, 8400 M^{-1} cm^{-1} at 254 nm for [poly(dG-dC)]$_2$, and 36600 M^{-1} cm^{-1} at 360 nm for APF (Professor W. D. Wilson, personal communication). All measurements on the DNAs were performed in a buffer containing 10 mM NaCl and 0.25 mM Na_2EDTA with a pH of 7.0 at ambient temperature.

The mixing ratio, R, is defined as the concentration ratio between the drug and nucleic acid (DNA phosphate):

$$R = C_{APF}/C_{DNA} \quad (1)$$

Most of our measurements were carried out under conditions where the amount of uncomplexed drug was small and, consequently, the mixing ratio approximately equal to the binding ratio (r).

Film Preparation. PVA was dissolved in water (10% w/v) under mild heating (80 °C). Aliquots of 5 mL were taken and each mixed with 3 mL of aqueous APF. The aliquots were poured onto horizontal glass plates and were left to dry for about 24 h in a dust-free environment. The films were then removed with a spatula, mounted in a stretching device, and stretched mechanically, in the air from a hair dryer (80 °C), by a factor of 3–5. Prior to measurement the films were mounted in holders to prevent relaxation.

Linear Dichroism. Linear dichroism (LD), the absorption anisotropy of a sample, is defined as

$$LD = A_{\parallel}(\lambda) - A_{\perp}(\lambda) \quad (2)$$

where $A_{\parallel}(\lambda)$ and $A_{\perp}(\lambda)$ denote absorptions measured with plane polarized light, polarized parallel and perpendicular, respectively, to the orientation direction. To be able to measure LD, the sample has to be oriented. The strength of the LD signal depends on the orientation of the absorbing species, its molar absorptivity, and its concentration. To compensate for dependency on the latter quantities and on path length, a normalized quantity, the reduced linear dichroism (LD^r), is defined:

$$LD^r = LD/A_{iso} \quad (3)$$

where A_{iso} is the absorption of the corresponding isotropic sample. LD_i^r, for a single transition, i, in a sample with uniaxial orientation, is given by the relation (Nordén, 1978)

$$LD_i^r = \frac{\epsilon_{xi}(\lambda)S_{xx} + \epsilon_{yi}(\lambda)S_{yy} + \epsilon_{zi}(\lambda)S_{zz}}{1/3[\epsilon_{xi}(\lambda) + \epsilon_{yi}(\lambda) + \epsilon_{zi}(\lambda)]} \quad (4)$$

where the S_{jj}'s are the Saupe order parameters describing the orientation of the molecules and ϵ's are the diagonal elements of the molar absorptivity tensor (Nordén *et al.*, 1992). In the notation used the z axis is the molecular axis that shows the best orientation (largest S value), the y axis is the second best oriented axis, and the x axis is the axis with the lowest S value. In the APF molecule (Figure 1) the z axis is the symmetry long axis of the molecule, the y axis is the in-plane short axis, and the x axis is the axis perpendicular to the molecular plane. The maximum value that S_{zz} can reach is 1.0. The parameters are interconnected through the equation $S_{xx} + S_{yy} + S_{zz} = 0$. For overlapping transitions the observed LD^r is a weighted average of the contributing transitions:

$$LD^r = \frac{\sum \epsilon_i(\lambda)(LD_i^r)}{\sum \epsilon_i(\lambda)} \quad (5)$$

The polarized spectra of APF in PVA film were measured on a CARY 2300 spectrophotometer with two Glan quartz polarizers inserted into the sample and reference beams. The spectra were recorded on a PC-AT IBM compatible computer connected to the spectrophotometer. A_{iso}, needed for LD^r, was calculated from the polarized spectra as (Nordén *et al.* 1992)

$$A_{iso}(\lambda) = (1/3)[A_{\parallel}(\lambda) + 2A_{\perp}(\lambda)] \quad \text{(uniaxial sample)} \quad (6)$$

The samples with APF bound to DNA were oriented in a shear flow field using a Couette cell with an outer rotating cylinder (Nordén *et al.*, 1992). The measurements were performed on a Jasco J-500 dichrometer modified and calibrated for LD measurements (Nordén & Seth, 1985), and the spectra were recorded on a PC-AT IBM compatible computer. A_{iso} was measured on the CARY 2300.

For orientation of DNA in a flow field one has (Nordén *et al.* 1992)

$$LD^r = S(3/2)(3\langle\cos^2\alpha\rangle - 1) \quad (7)$$

where S is an orientational function such that $S = 1$ denotes perfect orientation and $S = 0$ random orientation. $\langle\cos^2\alpha\rangle$ is an average representing static and dynamic variations of the local geometry; α denotes the angle between the transition moment and the DNA helix. For the DNA bases in B-form fiber DNA the effective value of α is 86° (Matsouka & Nordén, 1982).

Fluorescence Anisotropy. The fluorescence anisotropy (FA) of APF dissolved in 1,2-propanediol glass at 100 K was measured on an Aminco SPF-500 corrected spectra spectrofluorimeter. Emission intensity was measured with the polarizers set either vertically (V) or horizontally (H) in

incoming and outgoing light beams. The FA was calculated as

$$FA(\lambda) = \frac{I_{VV}(\lambda) - I_{VH}(\lambda)G(\lambda)}{I_{VV}(\lambda) + 2I_{VH}(\lambda)G(\lambda)} \quad (8)$$

where $G(\lambda) = I(\lambda)_{HV}/I(\lambda)_{HH}$ provides an instrument correction. The first index refers to the excitation polarizer and the second to the emission polarizer. The theoretical maximum anisotropy, +0.4, is reached for parallel absorbing and emitting transition moments when no reorientation of the molecules occurs during the fluorescence lifetime. If the requirement of no reorientation is fulfilled, the anisotropy of a pure transition is related to the angle, β_i, between the ith transition moment of absorption and the emission moment of the lowest energy transition as

$$FA_i = \frac{(3\cos^2\beta_i - 1)}{2} \times 0.4 \quad (9)$$

Circular Dichroism. Circular dichroism (CD) is defined as

$$CD = A(\lambda)_l - A(\lambda)_r \quad (10)$$

where $A(\lambda)_l$ and $A(\lambda)_r$ are the absorptions of left- and right-handed circularly polarized light, respectively. When normalized with respect to concentration and path length, this can be expressed as the difference in molar absorptivities of left- and right-handed circularly polarized light: $\Delta\epsilon = \epsilon(\lambda)_l - \epsilon(\lambda)_r$. APF itself is achiral, but when bound to DNA the drug chromophore acquires CD. If a single transition moment contributes, the CD profile is expected to have the same shape as the absorption profile (Cantor & Schimmel, 1980). The CD spectra were recorded on either a Jasco J-500 or a Jasco J-720 dichrometer.

Quantum Mechanical Calculation. Semiempirical MO calculations were carried out on a Micro VAX II using a CNDO/S standard program (Pople *et al.*, 1965; Delbene & Jaffe, 1968). The two-center electron repulsion integrals were calculated by the Mataga–Nishimoto scheme (Nishimoto & Mataga, 1957). Configuration interactions between the 250 lowest singly excited states were included in the CI. Calculations on both the free base and the divalent cation, having the amidino groups protonized, were carried out. As an input geometry for the 2-phenylfuran part a crystal structure of ethyl 2-acetyl-3-[5-(*p*-tolyl)-2-furyl]acrylate (Lokaj *et al.*, 1990) was used, and the molecular geometry of the amidino groups was taken from the structure of *N*-(*p*-nitrophenyl) benzamidine (Surma *et al.*, 1988). For the divalent cation all four C–N bonds were taken to be equal to 1.32 Å, the average value for the two C–N bonds in the unprotonated amidine group. All C–H and N–H bonds were taken to be 1.08 Å. Although the crystal structure of the substituted benzamidine shows a dihedral angle of 21° between the phenyl ring and the amidino group (Surma *et al.*, 1988), the calculations were made on planar geometries. Calculations with the amidinium groups twisted by 20° resulted in a blue shift of the lowest transition by about 5 nm, but no other significant differences from the planar conformation were noted.

RESULTS

Assignments of Transitions. 2,5-Bis(4-amidinophenyl)furan (APF) consists of a central furan ring with two phenyl rings symmetrically attached in the 2 and 5 positions (Figure 1). Each phenyl has an auxochromic amidino group in the 4 position. Due to the high pK_a of the amidino group, 11.6 for benzamidine (Albert *et al.*, 1947), these can be assumed

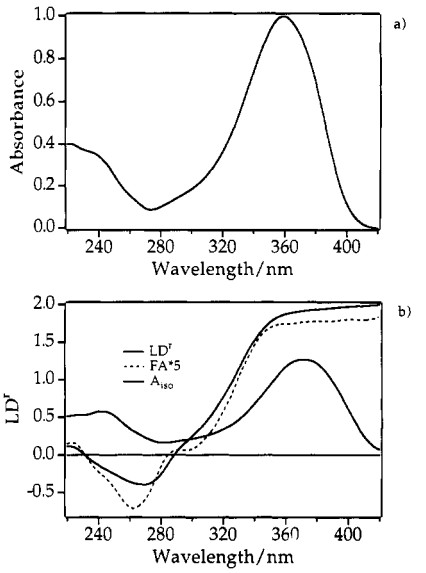

FIGURE 2: (a) Absorption spectrum of 2,5-bis(4-amidinophenyl)furan (APF) in water. (b) Polarized spectra of APF: reduced linear dichroism (LD^r) and absorption in a stretched PVA film and fluorescence anisotropy (FA) in 1,2-propanediol glass at 100 K. These spectra indicate that the absorption band at 340–400 nm arises from a single electronic long axis polarized transition.

to be protonated in aqueous solution. In its planar conformation the chromophore has C_{2v} symmetry, implying that any $\pi \rightarrow \pi^*$ transition must be polarized along either of the in-plane symmetry axes, denoted y and z in Figure 1. The absorption spectrum of APF in water shows a broad absorption maximum centered at 360 nm (Figure 2a) and in stretched PVA at 370 nm (Figure 2b), and in 1,2-propanediol glass at low temperature the band shows a pronounced vibrational structure with a maximum at 395 nm (not shown). The LD spectrum of APF when aligned in a stretched PVA film (Figure 2b) displays a large positive LD^r, +1.96, essentially constant over the 350–400-nm absorption band, indicating a single transition polarized parallel to the long axis of the molecule. Below 340 nm, several overlapping transitions of different polarizations are evidenced from the curvature of the LD^r profile. For a pure transition (no overlapping absorption from other transitions) the orientation parameter can be calculated directly from LD^r according to eq 4: $LD_i^r = 3S_{jj}$. In the case of APF this yields $S_{zz} = +0.67$ which is a reasonable value regarding the shape and size of this molecule (Nordén, 1978, 1980).

The fluorescence anisotropy (FA), as a function of the wavelength, closely resembles the LD^r curve. The maximum at 400 nm, +0.35, is just slightly less than the theoretical value +0.40.

In contrast to DAPI for which two strong bands of opposite signs are observed in the MCD spectrum at the position for the long-wavelength absorption band (Kubista *et al.*, 1989), which provides strong evidence for the existence of two close-lying nonparallel transitions in that case (Nordén *et al.*, 1992), APF shows just one weak band (results not shown), indicating a single transition only (Håkansson *et al.*, 1977; Nordén *et al.*, 1978; Albinsson *et al.*, 1990).

The quantum mechanical calculations (Table I) fully support the conclusions from the spectroscopic results. They predict the lowest-energy transition of the diprotonated form of APF to be polarized purely along the long axis of the molecule and situated at 404 nm. The next transition has a short axis polarization and is predicted to occur at 335 nm, in agreement with the FA and the stretched film LD results. Its oscillatory strength is calculated to only about one-eighth

Table I: CNDO/S Calculations on the APF Chromophore

transition no.[a]	wavelength (nm)	oscillator strength	polarization
	A. Divalent Cationic Form		
1	404	0.973	*z*
2	335	0.122	*y*
8	248	0.052	*y*
9	233	0.090	*y*
10	229	0.174	*z*
22	197	0.077	*y*
25	192	0.359	*z*
	B. Uncharged Form		
1	354	0.795	*z*
5	286	0.176	*x*
6	286	0.123	*y*
7	244	0.124	*y*
10	227	0.055	*y*
11	225	0.069	*y*
21	200	0.068	*y*
22	198	0.156	*z*
24	192	0.290	*y*

[a] Only transitions predicted to occur above 190 nm and to have oscillator strengths larger than 0.05 have been included.

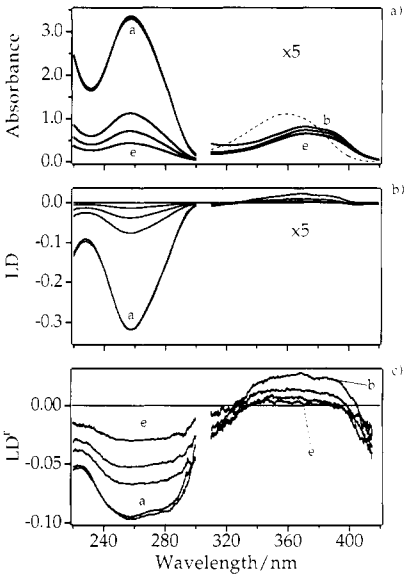

FIGURE 3: (a) Absorption, (b) LD, and (c) LD^r of 5.5 μM APF bound to calf thymus DNA. The dashed line shows the absorption of the drug in the absence of DNA. Drug/DNA phosphate ratios are (a) 0 (DNA concentration 0.55 mM) (b) 0.01, (c) 0.03, (d) 0.05, and (e) 0.1. The positive LD at the long-wavelength absorption of the chromophore implies that the compound is not intercalated. The LD^r analysis gives an angle of 46° ± 2° between the long axis (z) of APF and the DNA helix axis. This is consistent with a minor-groove AT type of binding geometry [pitch angle 45°, Larsen *et al.* (1989)]. The negative LD at high binding ratios in the low-energy end of the spectrum could be due to a GC type of binding.

of that of the lowest-energy transition. At shorter wavelengths the calculations predict additional transitions with varying polarizations; however, here the experimental results are uncertain. It may be noted that a simple MO calculation on 2,5-diphenylfuran (Simon & Balaban, 1963), the parent compound of APF, does not indicate more than one transition in the low-energy band.

Binding to DNA and Polynucleotides. The isotropic absorption spectrum of APF shows a hypochromic effect and a red shift when the drug is complexed with double-helical DNA or polynucleotides. In calf thymus DNA (Figure 3) and $[poly(dA\text{-}dT)]_2$ (Figure 4) the hypochromicity is about 20% while in $[poly(dG\text{-}dC)]_2$ (Figure 5) the effect amounts to about 40%. As the binding ratio is increased the absorption gradually decreases and is blue-shifted. The absorption profile does not change significantly between low and intermediate

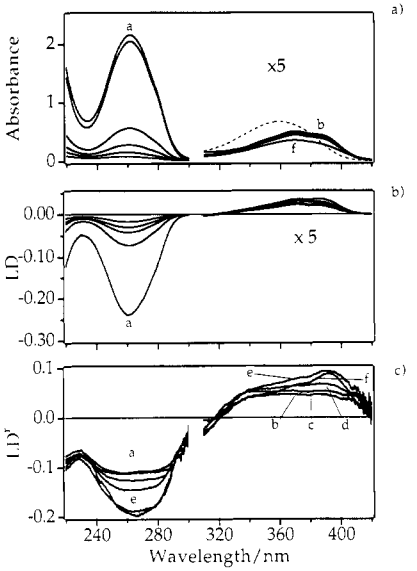

FIGURE 4: (a) Absorption, (b) LD, and (c) LD^r of 4 μM APF bound to $[poly(dA\text{-}dT)]_2$. The dashed line shows the absorption of the drug in the absence of DNA. Drug/DNA phosphate ratios are (a) 0 ($[poly(dA\text{-}dT)]_2$ concentration 0.40 mM), (b) 0.01, (c) 0.04, (d) 0.092, (e) 0.195, and (f) 0.4. The LD^r behavior of APF is similar to that of DAPI bound to $[poly(dA\text{-}dT)]_2$ (Nordén *et al.*, 1990). The angle between the long axis of APF and the DNA helix axis is found to be 46° ± 2°. The wavelength dependence at high binding ratios in the LD^r possibly originates from ligand–ligand interaction.

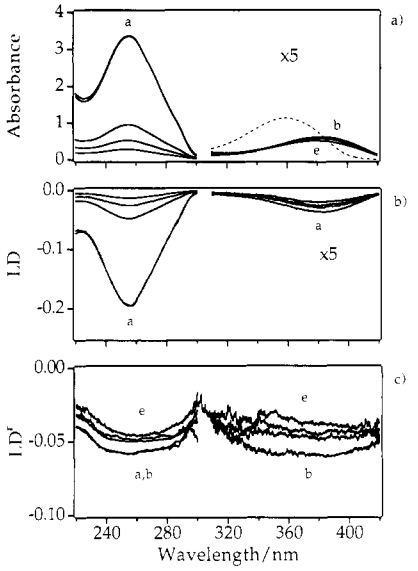

FIGURE 5: (a) Absorption, (b) LD, and (c) LD^r of 5.5 μM APF bound to $[poly(dG\text{-}dC)]_2$. The dashed line shows the absorption of the drug in the absence of DNA. Drug/DNA phosphate ratios are (a) 0 (DNA concentration 0.55 mM), (b) 0.01, (c) 0.04, (d) 0.08, and (e) 0.16. The absorption maximum is blue-shifted with anincreasing binding ratio. APF binds to $[poly(dG\text{-}dC)]_2$ with its long axis parallel to the DNA bases.

binding ratios. When added to $[poly(dA\text{-}dT)]_2$, the absorption of APF is constant up to higher binding ratios than it is in the complexes with calf thymus DNA and $[poly(dG\text{-}dC)]_2$.

The LD displayed in the first absorption band of APF upon binding to flow-oriented calf thymus DNA and $[poly(dA\text{-}dT)]_2$ is positive (Figures 3 and 4). By contrast, when the drug binds to $[poly(dG\text{-}dC)]_2$, the LD is negative (Figure 5).

After the LD^r for APF bound to $[poly(dA\text{-}dT)]_2$ is calculated as a function of the wavelength, it can be seen that the LD^r profile resembles that of DAPI bound to $[poly(dA\text{-}dT)]_2$ (Nordén *et al.*, 1990). The angle of orientation, at ratios below 0.1, calculated from LD^r using eq 7 corresponds to 46°

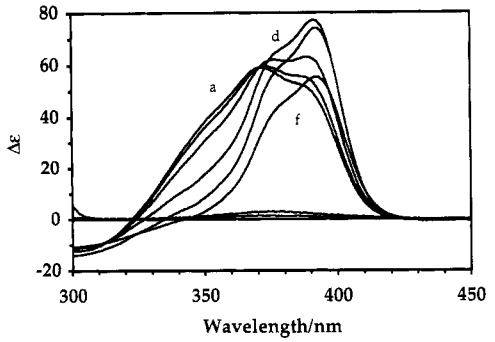

FIGURE 6: CD titration of APF bound to $[poly(dA\text{-}dT)]_2$ and $[poly(dG\text{-}dC)]_2$. The drug/DNA phosphate ratios for APF bound to $[poly(dA\text{-}dT)]_2$ are (a) 0.01, (b) 0.02, (c) 0.04, (d) 0.08, (e) 0.16, and (f) 0.31. The CD of APF bound to $[poly(dG\text{-}dC)]_2$ (the lower signals) is about an order of magnitude lower than the signal upon binding to $[poly(dA\text{-}dT)]_2$. At low binding ratios the CD of APF bound to $[poly(dA\text{-}dT)]_2$ has a maximum intensity around 270 nm and a shoulder around 390 nm. Increasing binding ratios shift the CD maximum to higher wavelengths. This behavior with two CD modes is similar to that of DAPI. At a binding ratio of about 0.16 the signal starts to decrease due to other types of binding than minor-groove binding.

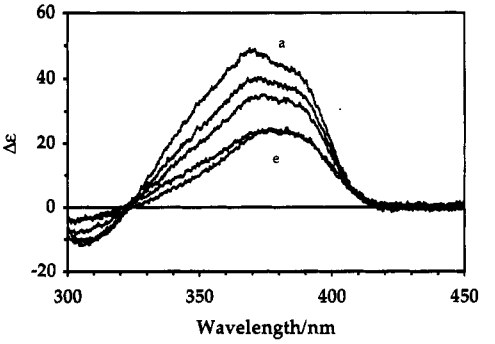

FIGURE 7: CD titration of APF bound to calf thymus DNA. The drug/DNA phosphate ratios are (a) 0.01, (b) 0.03, (c) 0.05, (d) 0.1, and (e) 0.2. At low binding ratios the CD resembles that of the drug bound to $[poly(dA\text{-}dT)]_2$. At high ratios the CD is more like that of binding to $[poly(dG\text{-}dC)]_2$.

± 2° between the long axis of APF and the DNA helix axis (within a couple of degrees the same angle obtained in the DAPI–$[poly(dA\text{-}dT)]_2$ complex), which is consistent with a minor-groove binding geometry [45° in the crystal structure by Larsen *et al.* (1989)]. The increasing amplitude of the LD^r signal in the DNA band, which implies an increased S value, indicates an increase of the persistence length of the DNA chain with increasing binding ratio (at low binding ratios the absorption of APF can be neglected compared with the absorption of DNA). Such a stiffening has also been observed when DAPI binds to $[poly(dA\text{-}dT)]_2$ and has been ascribed to a steric effect as the drug molecule is filling up the groove (Nordén *et al.*, 1990). At low binding ratios the signal is essentially independent of the wavelength over the long-wavelength absorption band in agreement with the assumption that it originates from a single transition. At high binding ratios, on the other hand, a significant wavelength dependence is observed, the origin of which we shall return to.

The LD^r value for the drug bound to calf thymus DNA gives within experimental errors the same angle to the helix axis at low binding ratios as the binding to $[poly(dA\text{-}dT)]_2$ did: 46° ± 2°. The same profile over the low-energy band is observed at low and intermediate binding ratios. In addition, at higher binding ratios also a negative LD contribution in the long-wavelength edge of the spectrum can be seen (Figure 3).

Upon binding APF to $[poly(dG\text{-}dC)]_2$ (Figure 5) its spectroscopic behavior again resembles that of DAPI (Nordén *et al.*, 1990). The negative LD at 370 nm yields an LD^r value which at low binding ratios equals the LD^r of the DNA bases at 260 nm. This indicates that the DNA bases and the long axis polarized transition of the drug are parallel to each other. The LD^r in the DNA decreases in amplitude with the binding ratio, suggesting that the binding leads to a more flexible structure, *i.e.*, a behavior that is opposite to that of the complex with $[poly(dA\text{-}dT)]_2$. With a higher binding ratio there is also an apparent wavelength dependence in the LD^r spectrum over the region 300–400 nm (Figure 5).

APF exhibits an induced circular dichroism when complexed with polynucleotides that again shows large similarities with that of DAPI. At low binding ratios the induced CD of APF bound to $[poly(dA\text{-}dT)]_2$ (Figure 6) shows a positive maximum at about 370 nm with a shoulder at about 390 nm. Following the notation of the DAPI spectra (Manzini *et al.*, 1983; Kubista *et al.*, 1987), this spectrum will be called a "mode I" spectrum. As the binding ratio increases the maximum is shifted to about 390 nm with a shoulder at 370 nm. The new component in the spectrum may be denoted the "mode II" spectrum in analogy with the DAPI case (Nordén *et al.*, 1990). At very high binding ratios the intensity, which is normalized with respect to the total amount of drug, decreases noticeably possibly due to something other than minor-groove binding modes and to some occurrence of uncomplexed drug. Also when APF is complexed with $[poly(dG\text{-}dC)]_2$, the induced CD is positive (Figure 6), however, an order of magnitude smaller than in the complex with $[poly(dA\text{-}dT)]_2$. The CD of APF when bound to calf thymus DNA (Figure 7) has the same profile as APF bound to $[poly(dA\text{-}dT)]_2$ at low binding ratios, but the intensity is significantly lower. At higher binding ratios the spectra resemble those of APF bound to $[poly(dG\text{-}dC)]_2$, suggesting that GC sequences of DNA are populated. The behavior with two apparent modes is not seen when APF is complexed with $[poly(dG\text{-}dC)]_2$.

DISCUSSION

Just One Pure Long Axis Polarized Electronic Transition Is Responsible for the Low-Energy Absorption Band of APF. Since this is an assignment of great importance for the structural interpretation of the spectra of the DNA complexes with APF, and for parallel inferences about DAPI too, let us consider the evidence for it. The LD^r value for APF oriented in a film is high, positive, and almost constant over the absorption band. A high value is expected for a rodlike molecule orienting well in a uniaxial matrix (Nordén, 1978). The positive sign and the fact that the LD^r profile is practically constant are consistent with a single transition polarized parallel to the long axis of the molecule; the constant FA behavior also supports the pure polarization. The high symmetry of the APF compound, effectively C_{2v}, implies that any transition must be polarized along either of the three mutually orthogonal symmetry axes (Cotton, 1971). The weak MCD that does not change sign (Håkansson *et al.*, 1977; Albinsson *et al.*, 1990), the constant LD^r profile at low binding ratios when binding to DNAs (Nordén *et al.*, 1992), and the fact that the CD profiles and absorption profiles, at low binding ratios, have the same shape (Cantor and Schimmel, 1980) are other observations strongly indicating only a single transition in the low-energy band of APF. From the theoretical calculations it is also clear that there is only one isolated transition in the low-energy region. This result is in contrast to the calculations on 2-phenylindole, the parent chromophore of DAPI, which exhibits two transitions in its low-energy band (Albinsson *et al.*, 1991), supporting the assumption that DAPI has two transitions. As will be returned to, the two transitions

coincide with the two DNA-induced circular dichroism bands, characteristic of the two binding modes of DAPI to AT stretches, and have therefore been taken as prerequisite for this behavior of DAPI (Kubista *et al.*, 1987). In APF at wavelengths shorter than 340 nm the LD^r and FA both suggest the presence of several transitions with varying polarizations at higher energies. Also these conclusions are supported by the theoretical calculations.

APF Is an AT-Specific Minor-Groove Binder. This conclusion can be drawn from the strong similarity between DAPI and APF, in agreement with findings by Wilson *et al.* (1990b). Both compounds have binding geometries in which their long axes are close to 45° to the helix axis in calf thymus DNA (Kubista *et al.*, 1987) and $[poly(dA\text{-}dT)]_2$ (Nordén *et al.*, 1990). However, when complexed with $[poly(dG\text{-}dC)]_2$ (Nordén *et al.*, 1990), both compounds bind in a manner such that their long axes are parallel to the DNA bases, an orientation consistent with intercalation (Wilson *et al.*, 1990a) or a binding mode in which the drug is bound in the major groove with the in-plane short axis more or less parallel with the DNA helix axis (Eriksson *et al.*, 1993; Kim *et al.*, 1993).

The strong and positive induced CD of DAPI in AT environments, which shifts to a "second mode" spectrum with increasing binding ratio, is a behavior also found for APF. The strongly positive CD spectrum of APF upon binding to AT regions can be rationalized as induced CD in an electric dipole allowed transition with a moment directed along a groove. Recent calculations (Lyng *et al.*, 1991, 1992) show that such a CD will be strongly positive whether the ligand binds in the minor or the major grooves of the B form $[poly(dA\text{-}dT)]_2$. Therefore, CD cannot *per se* be used to discriminate in which groove the ligands are bound. However, regarding the great similarities (Wilson *et al.*, 1990b), in both binding properties and binding geometries, between DAPI and APF, it seems justified to conclude that the latter too is an AT-specific minor-groove binder in its high-affinity binding mode. The drop in LD^r at wavelengths below 340 nm, in the region where the DNA bases have no absorption, indicates that the short axis transition of APF in this region is oriented perpendicular to the DNA helix axis in agreement with a groove binding geometry such that DAPI be edgewise inserted. A minor-groove binding would for steric reasons give a rather precise orientation of the in-plane short axis of APF perpendicular to the DNA helix axis whereas major-groove geometries are likely to give, on average, large inclinations away from perpendicularity.

By contrast to the AT binding geometry, the geometry in $[poly(dG\text{-}dC)]_2$ with the long axis of the drug oriented parallel to the bases is consistent with APF being intercalated in an alternating GC sequence (Wilson *et al.*, 1990b). This orientation is also consistent with binding in the major groove, a mode that has been proposed for DAPI binding to alternating GC sequences (Eriksson, 1992; Kim *et al.*, 1993). The short axis in-plane polarized transition of APF provides a possibility to probe the orientation of the short axis in the complex. In the case of intercalation also this transition should be perpendicular to the helix axis, *i.e.*, have an LD^r close to that of the DNA bases. However, as can be observed in Figure 5c this is not the case, but the less negative LD^r instead suggests that the short axis transition is significantly tilted, contradicting classical intercalation.

With calf thymus DNA APF is an AT minor-groove binder at low ratios. This is concluded from LD^r at 370 nm, giving an angle of about 45° to the helix axis, and from the observation of strong positive CD for the same transition. At high binding ratios there is a drop in LD and, in the long-wavelength edge of the spectrum, a sign change to a negative LD signal. The same type of behavior has been seen also in the LD spectrum for DAPI bound to DNA (Eriksson, 1992, Kim *et al.*, 1993). This negative LD^r can be interpreted in terms of the presence of some perpendicularly oriented drug molecules at high binding ratios, reflecting pure GC environments in DNA. The behavior in absorption also supports this hypothesis as does the circular dichroism: the CD of APF bound to DNA is of "AT mode I" type at low binding ratios but turns into a more GC-like spectrum at higher ratios (Figure 7). DAPI is known to bind strongly also to alternating GC sequences, and the same obviously holds for APF too (Wilson *et al.*, 1990b).

The Two Modes Seen by CD Are Not Related to Different Transitions. The CD behavior of APF bound to $[poly(dA\text{-}dT)]_2$ closely resembles that of DAPI (Manzini *et al.*, 1983; Kubista *et al.*, 1987; Nordén *et al.*, 1990), both showing a switch from mode I to mode II with increasing binding ratio. In the case of DAPI this behavior has been proposed to be related to the enhancement of either of the two low-energy transitions in the DAPI chromophore, both nearly long axis polarized but with some 15° divergence between them (Kubista *et al.*, 1989). However, since there is clearly only a single transition in APF, in this energy region, and the CD spectra of the two drugs strongly resemble each other, including the mode II behavior, we conclude that the respective spectral effects of the two modes are not related to whether there are two transitions in the chromophore.

Is the "Mode II" CD an Exciton Effect between Adjacent Ligands? Careful comparison of LD^r and CD spectra between DAPI and APF reveals the same kind of behavior. The LD^r spectra of both drugs when bound to $[poly(dA\text{-}dT)]_2$ exhibit a constant profile for binding ratios lower than 0.05. When the binding ratios come between 0.05 and 0.1, distinct changes in the profiles are seen. In the long-wavelength end of the spectrum there is an increase in the signal (more positive) compared with the signal at short wavelengths. A question that must be critically considered is whether this might be an artifact due to uncomplexed drug contributing in A_{iso} but not in LD. However, the high binding constant and a changing LD spectrum (LD sees only bound chromophores) proves that this is not the case but that the LD^r profile of the bound species indeed changes with the binding ratio. This could be a result of a changed binding geometry which, *e.g.*, could be the indirect effect of a changed DNA conformation. Another possibility, to which we shall return, is that the LD^r profile changes because of ligand–ligand interactions at higher binding ratios.

The CD spectra show a constant profile as long as the binding ratio is lower than 0.01; however, above this ratio mode II starts to show up. Above binding ratios of about 0.15 the CD signal, which is normalized with respect to the total drug concentration, starts to decrease. This decrease is only to a minor degree a result of the appearance of free drug.

Footprinting studies suggest that 3–4 base pairs are needed for DAPI to bind in the AT mode (Jeppesen & Nielsen, 1989; Portugal & Waring, 1988). Manzini *et al.* (1983) have estimated the site size to be three base pairs. This site size probably holds also for APF with its amidino groups at the ends and nearly the same length. Assuming that each drug molecule needs three base pairs to bind in its high affinity mode, the minor groove would be crowded at a binding ratio of about 0.17. Therefore, at higher ratios the mode of binding must be other than minor-groove binding. Calculations (Lyng *et al.*, 1991, 1992) indicate that any other binding modes than groove modes would exhibit considerably lower CD which

can explain the experimentally observed decrease in the overall signal above a binding ratio of 0.15.

The maximum intensity of the mode II CD occurs at the same wavelength at which the most positive peak appears in the LD^r spectrum at high binding ratios. This positive LD^r peak, at the long-wavelength side of the absorption, could be the low-energy in-phase exciton component of two drug molecules interacting in a head–tail manner in the minor groove. The LD for an interaction of this kind is given by the resultant transition moment (Nordén *et al.*, 1992), which for a geometry of 2 drug units per 2/3 turn of the groove will lie at an angle α around 30°, in qualitative agreement with a more positive LD^r. A "two-mode" behavior is also seen in the CD spectra of the antibiotic drug netropsin (Zimmer & Wähler, 1986) as well as for Hoechst 33258 (Jorgenson *et al.*, 1988). The fact that the phenomenon is common to three so structurally different minor-groove binders seems to exclude that it is a unique property of the DAPI chromophore due to some specific, subtle conformational change in the drug, which has been one of the possibilities considered (Nordén *et al.*, 1990). Indeed, these observations support our hypothesis that the second CD mode is merely a result of interacting ligand chromophores, in which case the only requirement for a common behavior is the minor-groove geometry and the presence of a long axis polarized transition in the drug. If there had been two transitions in the low-energy band of APF, the CD behavior could have been the result of a change in the environment as previously proposed for DAPI. However, since there is only one transition in APF and the CD spectra resemble those of the DAPI complexes, the two-transition explanation can be dismissed.

The CD spectra of strong electric dipole transitions more sensitively reflect (degenerate) ligand–ligand interactions and are anticipated to show a change in profile at an earlier stage than the LD spectrum does upon increasing binding ratios. This is so because degenerate exciton CD of coupled oscillators at a given distance from each other is 1 or 2 orders of magnitude stronger than the nondegenerate CD, such as the DNA-induced CD in monomeric drug molecules (Jackson & Mason, 1971; Nordén *et al.* 1992). Methyl green, another groove binding dye (Krey, 1980), clearly shows a similar behavior with the effect of accidental dimers visible long before they appear in LD (Nordén *et al.*, 1978; K. Jansen, unpublished results).

An allosteric model for the binding to DNA has been proposed for both DAPI (Wilson *et al.*, 1990a) and APF (Wilson *et al.*, 1990b) on the basis of binding studies performed with dialysis. The allosteric model means that, as the drug binds, the DNA structure is altered so that binding of further drug molecules is facilitated. The occurrence of the mode II CD has been considered as a possible result of the allosteric effect in that the DNA structure, and thus the induced CD, might be different when several drug molecules are bound compared to single ones (Nordén *et al.*, 1990; Eriksson *et al.*, 1993). Since the energy of the drug transition will not depend on the DNA conformation, a minor conformational change in the drug would in this mechanism also be necessary to assume. However, against what has been said above we consider this mechanism highly improbable regarding the similar behaviors of DAPI, APF, Hoechst 32258, and netropsin.

In conclusion, the results presented here clearly show that an allosteric conformational change is not needed to explain the mode II CD spectrum of APF. Eriksson *et al.* (1993) have analyzed the CD spectra of DAPI–DNA mixtures using a chemometric technique and conclude from their analysis that the experimental data could be explained equally well by "accidental dimers" as by an allosteric binding model. Accidental dimer was coined to denote two chromophores, within a statistical distribution of DNA-bound ligands, that just happen to bind close to each other (Nordén & Tjerneld, 1982). The model with accidental dimers was considered unlikely by Eriksson *et al.* (1993) on the basis of DAPI's divalent charge. However, at binding ratios lower than 0.2, *i.e.*, one ligand per five bases, still only less than half of the negative charge of DNA is neutralized by a dicationic ligand. Furthermore, Manzini *et al.* (1983) have shown that the binding constants for both modes of binding are sensitive to ionic strength and that the binding constant for mode II decreases even more with increasing ionic strength than the binding constant for mode I does. It is difficult to see how the second, main stage of the allosteric binding model should be extra salt sensitive if it were based on free-energy release owing to a DNA conformational change.

A statistical-thermodynamical estimate based on the allosteric model indicates that as many as 100–500 base pairs might be brought into a new conformational change by three contiguously bound DAPI molecules (Eriksson *et al.*, 1993). The number of base pairs that are changed depends on the parameters used. Using the McGhee–von Hippel equation for ligands bound without cooperativity (McGhee & von Hippel, 1974), the binding ratio, at which 10% of the ligands bound are bound with three or more ligands in contigue, is reached at a binding ratio of 0.12. Although a model without cooperativity probably does not describe the system in a correct way, it can give a hint about how the system might work. At this binding ratio the whole DNA would be in the altered state. By contrast the CD signal at constant drug concentration continues to increase above this binding ratio, an observation that again contradicts the allosteric model.

CONCLUSIONS

What has been learned from this study may be summarized as follows.

(1) Linear dichroism, fluorescence anisotropy, and quantum mechanical calculations clearly show that the absorption band at 340–400 nm in APF is due to an isolated $\pi \rightarrow \pi^*$ transition polarized parallel to the z symmetry axis. The next transition, around 330 nm, is y-polarized.

(2) From this information the flow linear dichroism spectra of APF complexes with nucleic acids can be interpreted in terms of distinct binding geometries. In calf thymus DNA (at low binding ratios), as well as $[poly(dA\text{-}dT)]_2$, APF is edgewise inserted into the minor groove with an angle of 46° ± 2° of its z axis relative to the DNA helix axis and with its y axis perpendicular to the helix. In $[poly(dG\text{-}dC)]_2$ the z axis lies close to 90° as expected for intercalation; however, a tilted y axis seems to exclude intercalation. In $[poly(dA\text{-}dT)]_2$, APF makes the double helix stiffer, whereas in $[poly(dG\text{-}dC)]_2$ APF leads to a decreased persistence length, again contradicting classical intercalation.

(3) In the circular dichroism spectrum of APF–$[poly(dA\text{-}dT)]_2$ the appearance of a second, strongly positive mode II band at 390 nm at binding ratios above 0.01 drug/DNA phosphate is found to be due to exciton interactions. Linear dichroism indicates that the binding geometry is not significantly changed with increasing binding ratio. Linear dichroism also suggests that the exciton interaction occurs between the mode I minor-groove bound APF molecules when they accidentally come closer to each other.

(4) There is a striking similarity between APF and DAPI as to the respective binding geometries in DNA, $[poly(dA\text{-}dT)]_2$, and $[poly(dG\text{-}dC)]_2$, but also spectroscopic details such

as exciton evidence in linear dichroism as well as the appearance of a mode II circular dichroism with increasing binding ratio. Taken together all evidence suggests that, in DAPI too, the explanation of mode II is just an exciton effect between long axis transitions of the minor-groove bound chromophore. Finally the fact that the pitch angle of the double helix, within an error of a few degrees, remains around 46° also at higher binding ratios is an argument against allosteric binding models invoking conformational change of the nucleic acid.

ACKNOWLEDGMENTS

We are grateful to Professor W. D. Wilson for valuable discussions and for providing us with APF, a gift from Drs. B. P. Das and D. W. Boykin.

REFERENCES

Albert, A., Mills, J. A., & Royer, R. (1947) *J. Chem. Soc.* 1452.
Albinsson, B., Eriksson, S., Lyng, R., & Kubista, M. (1991) *Chem. Phys. 151*, 149–157.
Albinsson, B., Kubista, M., Sandros, K., & Nordén, B. (1990) *J. Am. Chem. Soc. 94*, 4006–4011.
Ashley, J. N., Barber, H. J., Ewins, A. J., Newbery, G., & Self, A. D. H. (1942) *J. Chem. Soc.* 103–116.
Bella, J. L., & Gosálvez, J. (1991) *Biotechnol. Histochem.* 44–52.
Bernheim, A., & Miglierina, K. (1989) *Hum. Genet. 83*, 189–193.
Brown, R. N., & Hitchcock, P. F. (1989) *Dev. Brain. Res. 50*, 123–128.
Cantor, C., & Schimmel, P. R. (1980) *Biophysical Chemistry Part II: Techniques for the study of biological structure and function*, W. H. Freeman and Co., New York.
Chi, H., Ishibashi, Y., Shima, A., Mihara, I., & Osuka, F. (1990) *J. Invest. Dermatol. 95*, 154–157.
Cotton, F. A. (1971) *Chemical Applications of Group Theory*, 2nd ed., Wiley-Interscience, New York.
Dann, O., Bergen, G., Demant, E., & Volz, G. (1971) *Liebigs Ann. Chem. 749*, 68–89.
Dann, O., Fick, H., Pietzner, B., Wallcenthorst, E., Fernbach, R., & Zed, D. (1975) *Liebigs Ann. Chem.* 160–194.
Das, B. P., & Boykin, D. W. (1977) *J. Med. Chem. 20*, 531–536.
Eriksson, S. (1992) Doctoral Thesis, Chalmers University of Technology, Göteborg, Sweden.
Eriksson, S., Kim, S. K., Kubista, M., & Nordén, B. (1993) *Biochemistry 32*, 2987–2998.
Festy, B., & Duane, M. (1973) *Biochemistry 12*, 4827–4834.
Festy, B., Strum, J., & Duane, M. (1975) *Biochim. Biophys. Acta 407*, 24–42.
Håkansson, R., Nordén, B., & Thulstrup, E. W. (1977) *Chem. Phys. Lett. 50*, 305–308.
Hajduk, S. L. (1976) *Science 191*, 858–859.
Jackson, K., & Mason, S. F. (1971) *Trans. Faraday Soc. 67*, 966–989.
Jeppesen, C., & Nielsen, P. E. (1989) *Eur. J. Biochem 182*, 437–444.
Jorgenson, K. F., Varshney, U., & van de Sande, J. H. (1988) *J. Biomol. Struct. Dyn. 5*, 1005–1023.
Kapuschinski, J., & Yanagi, K. (1979) *Nucleic Acids Res. 6*, 3535–3542.
Kim, S. K., Eriksson, S., Kubista, M., & Nordén, B. (1993) *J. Am. Chem. Soc.* (in press).
Krey, A. (1980) *Prog. Mol. Subcell. Biol. 7*, 43–87.
Kubista, M., Åkerman, B., & Albinsson, B. (1989) *J. Am. Chem. Soc. 111*, 7031–7035.
Kubista, M., Åkerman, B., & Nordén, B. (1987) *Biochemistry 26*, 4545–4553.
Larsen, T. A., Godsell, D. S., Cascio, D., Grezeskowiak, K., & Dickerson, R. E. (1989) *J. Biomol. Struct. Dyn. 7*, 477–491.
Lee, G. M., Thornwaite, J. T., & Rasch, E. M. (1984) *Anal. Biochem. 137*, 221–225.
Lin, M. S., Comings, D. E., & Alfi, O. S. (1977) *Chromosoma 60*, 15–25.
Lokaj, L., Vrábel, V., Sivy, P., Ilavsky, D., & Jecny, J. (1990) *Acta Crystallogr. C46*, 1558–1560.
Loontiens, F. G., McLaughlin, L. W., Diekmann, S., & Clegg, M. R. (1991) *Biochemistry 30*, 182–189.
Lyng, R., Rodgers, A., & Nordén, B. (1991) *Biopolymers 31*, 1709–1720.
Lyng, R., Rodgers, A., & Nordén, B. (1992) *Biopolymers 32*, 1201–1214.
Manzini, G., Barcellona, M. L., Avitabile, M., & Quadrifoglio, F. (1983) *Nucleic Acids Res. 11*, 8861–8876.
McGhee, J. D., & von Hippel, P. H. (1974) *J. Mol. Biol. 86*, 469–489.
Matsuoka, Y., & Nordén, B. (1982) *Biopolymers 21*, 2433–2452.
Newton, B. A. (1967) *Biochem. J.* P50–P51.
Nordén, B. (1978) *Appl. Spectrosc. Rev. 14*, 157–248.
Nordén, B. (1980) *J. Chem. Phys. 9*, 5032–5038.
Nordén, B., Håkansson, R., Pedersen, P. B., & Thulstrup, E. W. (1978) *Chem. Phys. 33*, 355–366.
Nordén, B., Eriksson, S., Kim, S. K., Kubista, M., Lyng, R., & Åkerman, B. (1990) in *Proceedings of the twenty-third Jerusalem symposium on quantum chemistry and biochemistry* (Pullman, B., & Jortner, J., Eds.) pp 32–41, Kluwer Academic Publishers, Dordrecht, The Netherlands.
Nordén, B., Kubista, M., & Kurucsev, T. (1992) *Q. Rev. Biophys. 1*, 51–179.
Nordén, B., & Seth, S. (1985) *Appl. Spectrosc. 39*, 647–655.
Nordén, B., & Tjerneld, F. (1982) *Biopolymers 21*, 1713–1734.
Nordén, B., Tjerneld, F., & Palm, E. (1978) *Biophys. Chem. 8*, 1–15.
Portugal, J., & Waring, M. J. (1988) *Biochim. Biophys. Acta 949*, 158–168.
Russel, W. C., Newman, C., & Williamson, D. H. (1975) *Nature 253*, 461–462.
Schwartz, D. C., & Koval, M. (1989) Nature *338*, 520–521.
Simon, Z., & Balaban, A. T. (1963) *Acad. Repub. Pop. Rom.* I.F.A-24.C0.
Surma, K., Jaskólski, M., Kosturkiewicz, Z., & Oszczapowicz, J. (1988) *Acta Crystallogr. C44*, 1031–1033.
Takata, K., & Hirano, H. (1990) *Acta Histochem. Cytochem. 23*, 679–683.
Tijssen, J. P. F., Beekes, H. W., & van Stevenick, J. (1982) *Biochem. Biophys. Acta 721*, 394–398.
Williamson, D. H., & Fenell, D. J. (1979) *Methods Enzymol. 56*, 728–733.
Wilson, W. D., Tanious, F. A., Barton, H. J., Jones, R. L., Fox, K., Wydra, R. L., & Strekowski, L. (1990a) *Biochemistry 29*, 8452–8461.
Wilson, W. D., Tanious, F. A., Buczak, H., Venkatramana, M. K., Das, B. P., & Boykin, D. W. (1990b) in *Proceedings of the twenty-third Jerusalem symposium on quantum chemistry and biochemistry* (Pullman, B., & Jortner, J., Eds.) pp 331–353, Kluwer Academic Publishers, Dordrecht, The Netherlands.
Zimmer., C., & Wähnert, U. (1986) *Prog. Biophys. Biol. 47*, 31–112.